

# Thermodynamic and dynamic anomalies for dumbbell molecules interacting with a repulsive ramplike potential

Paulo A. Netz,<sup>1</sup> Sergey V. Buldyrev,<sup>2,3</sup> Marcia C. Barbosa,<sup>4,\*</sup> and H. Eugene Stanley<sup>3</sup>

<sup>1</sup>*Instituto de Química, Universidade Federal do Rio Grande do Sul, Porto Alegre, RS, Brazil*

<sup>2</sup>*Yeshiva University, Department of Physics, 500 West 185th Street, New York, New York 10033, USA*

<sup>3</sup>*Center of Polymer Studies and Department of Physics, Boston University, Boston, Massachusetts 02215, USA*

<sup>4</sup>*Universidade Federal do Rio Grande do Sul, Caixa Postal 15051, 91501-970, Porto Alegre, RS, Brazil*

(Received 10 August 2005; revised manuscript received 25 March 2006; published 7 June 2006)

Using collision driven discrete molecular dynamics, we investigate the thermodynamics and dynamics of systems of 500 dumbbell molecules interacting by a purely repulsive ramplike discretized potential, consisting of  $n$  steps of equal size. We compare the behavior of the two systems, with  $n=18$  and  $n=144$  steps. Each system exhibits both thermodynamic and dynamic anomalies, a density maximum and the translational and rotational mobilities show anomalous behavior. Starting with very dense systems and decreasing the density, both mobilities first increase, reach a maximum, then decrease, reach a minimum, and finally increase; this behavior is similar to the behavior of SPC/E (Simple Point Charge-Extended) water. The regions in the pressure-temperature plane of translational and rotational mobility anomalies depend strongly on  $n$ . The product of the translational diffusion coefficient and the orientational correlation time increases with temperature, in contrast with the behavior of most liquids.

DOI: [10.1103/PhysRevE.73.061504](https://doi.org/10.1103/PhysRevE.73.061504)

PACS number(s): 64.70.Pf, 82.70.Dd, 83.10.Rs, 61.20.Ja

## I. INTRODUCTION

Recently much attention has focused on phase behavior of single-component systems comprised of particles interacting via core-softened potentials [1–9]. Core-softened potentials exhibit a repulsive hard core plus a softening region, which can be a linear or nonlinear repulsive ramp, a shoulder, a double (or multiple) attractive well, or combinations of all these features. These models were created with the purpose of constructing a simple two-body isotropic potential capable of describing some aspects of the anomalous behavior of complex fluids [10–12], such as maximizing density as a function of temperature, increasing isothermal compressibility upon cooling, and increasing molecular diffusivity with the increase of pressure [11]. It has been proposed some time ago that these anomalies might be associated with a critical point at the terminus of a liquid-liquid line, in the unstable supercooled liquid region [13]. The study of core-softened potentials generates models that are computationally (sometimes even analytically) tractable and that may retain some qualitative features of network forming fluids such as water.

Hemmer and Stell [14], using the method of Takahashi [15] proposed the possibility of a second critical point in addition to the normal liquid-gas critical point, for a one-dimensional system whose pairwise potential possesses a region of negative curvature with respect to separation distance in its repulsive core. Debenedetti *et al.* developed thermodynamic arguments to show that this type of potential can lead to density anomaly [16]. Stillinger and Stillinger [17] showed that a pure repulsive Gaussian core-softened potential produces both thermodynamic and dynamic anomalies, but no indication of the second critical point at positive temperatures.

A number of works investigated step potentials consisting of a hard core, a square repulsive shoulder and an attractive square well [3–6,18–24]. In two dimensions, such potentials have density and diffusion anomalies, a negatively sloped freezing line and possibly a second critical point in a deeply supercooled state inaccessible by simulations. In three dimensions, these potentials do not have dynamic and thermodynamic anomalies but possess a second [20] and sometimes a third [19] critical point, accessible by simulations in the region predicted by the hypernetted chain integral equation [5,25].

Jagla proposed a different version of the core-softened potential, the main element of which is a linear repulsive ramp [2]. These potentials show a region of density anomaly in the pressure-temperature plane and also display a liquid-liquid critical point, which can be located in a stable or metastable fluid region, depending on the choice of parameters [26]. The Rogers-Young [27] approximation, together with the mode coupling theory, reproduces these features analytically [28]. An attractive ramp [2,8,29] displays a normal gas-liquid critical point and also brings this second critical point into an accessible region of higher temperature.

An interesting issue, besides the thermodynamic anomalies, is the investigation of the dynamic anomalies, such as those exhibited by water. The translational diffusion coefficient  $D$  for a spherical particle solute of radius  $\sigma$  in a medium of shear viscosity  $\eta$ , is predicted by the Stokes-Einstein relation to be

$$D = \frac{k_B T}{6\pi\eta\sigma}. \quad (1)$$

The rotational autocorrelation time is predicted by the Debye-Stokes-Einstein relation to be

\*Electronic address: [marcia.barbosa@ufrgs.br](mailto:marcia.barbosa@ufrgs.br)

$$\tau_r = \frac{4\pi\eta\sigma^3}{3k_B T}. \quad (2)$$

Simulations of supercooled SPC/E water at constant temperature show that  $D$  increases as pressure  $P$  decreases, reaches a maximum at a density  $\rho_{D \max}$  and decreases until  $D$  reaches a minimum at  $\rho_{D \min}$  [11,30–32]. Further  $\tau_r$  has a minimum at  $\rho_{D \max}$  and a maximum at  $\rho_{D \min}$  [11,30–32], and the product  $\tau_r D$  is almost constant with density and temperature [30–32]. This constancy is still an open issue and needs to be resolved.

Combining Eq. (2) with Eq. (1) we see that the product  $\tau_r D$  is constant, which could explain the constancy of the product  $\tau_r D$  observed in the SPC/E [33] water. However, the hydrodynamic approximations used in both the Stokes-Einstein and the Debye-Stokes-Einstein relations are valid only if the size ratio between the solute and the solvent is large [34]. This is not the case of the self-diffusion of SPC/E water where the tracer particle has the same size as the other particles in the system, so hydrodynamic arguments cannot explain the constancy of  $\tau_r D$  observed in water [30–32].

Furthermore, for a number of supercooled liquids, experimental results show that there is a breakdown of the Stokes-Einstein relation close to the glass transition temperature  $T_g$  [35–37]. The translational diffusion close to  $T_g$  behaves as  $D \propto T/\eta^b$  with  $b < 1$  [35]. In this case, the product  $\tau_r D \propto \eta^{1-b}$  is not constant, but increases as the system is cooled [35]. Since water differs from other supercooled liquids by the presence of thermodynamic anomalies, the study of the relation between the thermodynamic and dynamic anomalies in water might shed some light on this problem. For SPC/E water, the region in the  $P$ – $T$  phase diagram where water has diffusivity anomalies defines a broad region, and the region where density anomalies can be found lies entirely inside the anomalous diffusivity region [11,30–32,38]. For SPC/E water, the product  $\tau_r D$  is approximately constant inside the entire region of the diffusivity anomaly.

The goal of our study is to test the hypothesis that the constancy of  $\tau_r D$  is the consequence of the diffusivity anomaly. To achieve this goal, we construct a simple model which has the thermodynamic and dynamic anomalies of water but also has rotational degrees of freedom, so that  $\tau_r$  can be investigated. We based our model on the Jagla repulsive ramp model which has the entire spectrum of water anomalies [28], including the correlation between the translational and orientation order parameters [39]. In order to create rotational degrees of freedom, we linked two ramp particles into a “dumbbell” by a permanent bond equal in length to the hard core diameter. Thus, in our model, the two monomers of the dumbbell touch each other with their hard cores as in rhombohedral crystal obtained in [28] near the high-pressure border of the diffusivity anomaly region. We keep the same choice of the ratio of the soft core to the hard core as in [28], since this ratio also reproduces the waterlike correlation of the translational and orientational order maps [40]. Since hard-core models cannot be easily treated with a continuous molecular dynamics, we discretized the ramp by a step-function consisting of many small steps and use the discrete molecular dynamic (DMD) algorithm as in [28].

First, we test whether the thermodynamic and dynamic anomalies are preserved for dumbbells and how their region

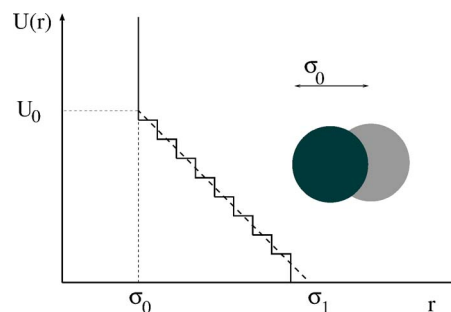


FIG. 1. (Color online) Purely repulsive ramp-like discretized potential consisting of  $n$  steps of equal size. Step potential (solid line) and comparison with the linear ramp (dashed line). Here,  $\sigma_0$  is the diameter of a spherical atom forming the dumbbell.

in the  $P$ – $T$  diagram is alternated comparatively to the original monomeric particles. Since in [28] it was shown that the dynamic properties depend significantly on the step of the discretized potential, we test our conclusions to determine whether or not they are an artifact of the discretization. Finally, in the density anomaly region, we can test if the product  $\tau_r D$  is constant (as in water) or if it resembles the behavior of other supercooled liquids.

This paper is organized as follows. We introduce the dumbbell model and give details about the simulations in Sec. II. We present the thermodynamic and dynamic behavior in Sec. III and our conclusions in Sec. IV.

## II. DUMBBELL MODEL

The model we study is defined as follows. We consider a set of diatomic molecules formed by two spherical atoms of diameter  $\sigma_0$  linked together. The atoms in each molecule are separated from each other by a distance  $\ell$  which is allowed to fluctuate in the range of  $0.99\sigma_0 \leq \ell \leq 1.01\sigma_0$ . The interaction potential between two atoms separated by a distance  $r$  belonging to different dumbbell molecules is a “ramp” made of  $n$  steps [28] (Fig. 1). Thus,

$$U(r) \equiv \begin{cases} \infty & r < \sigma_0 \\ k\Delta U & r_{k+1} < r < r_k \\ 0 & r > \sigma_1 - \frac{\Delta r}{2} \end{cases}, \quad (3)$$

where

$$r_k \equiv \sigma_1 - \left(k - \frac{1}{2}\right)\Delta r, \quad (4)$$

$$\Delta r \equiv \frac{\sigma_1 - \sigma_0}{n + (1/2)}, \quad (5)$$

and

$$\Delta U \equiv \frac{U_0}{n + (1/2)}. \quad (6)$$

The liquid phase part of the ramp phase diagram has the following characteristics. At low  $P$ , particles prefer to be at

distances  $\sigma_1$  from each other. At high  $P$ , the typical distance is  $\sigma_0$ . This implies a crossover region of  $P$  with anomalously large isothermal compressibility  $k_T$  which might give rise to an accessible liquid-liquid phase transition if an attractive part is included in this potential.

The discretized step version of the ramp potential has the advantage of being well suited for study using collision-driven molecular dynamics [20,41]. As  $n \rightarrow \infty$ , the step potential becomes a ‘‘ramp’’ similar to the potential introduced by Hemmer and Stell [14] and studied by Jagla [2]. Indeed, the properties become similar to a pure ramp potential if the height difference between two adjacent steps is less than  $k_B T$  [28]. Moreover, we expect [28] that the dynamic behavior converges to the behavior of the smooth ramp when  $n \rightarrow \infty$  as  $O(n^{-1})$ , therefore in a slower way than the thermodynamic properties, which converge as  $O(n^{-2})$ .

In order to test the influence of the discretization, we study this repulsive ramp potential with  $n=18$  and  $n=144$  steps and  $\sigma_1/\sigma_0=1.74$ . We perform DMD simulations, using a collision-driven algorithm [7,20,41], for a system comprised of 500 dumbbell molecules (1000 ‘‘atoms’’) in a cubic box, with box edge ranging from  $L=13\sigma_0$  to  $L=15.5\sigma_0$ . The dimensionless temperature  $T^*$ , density  $\rho^*$ , pressure  $P^*$ , translational diffusion coefficient  $D^*$ , and mean rotational correlational time  $\tau_r^*$  are given, respectively, by

$$T^* \equiv \frac{Tk_B}{U_0}, \quad (7)$$

$$\rho^* \equiv \rho\sigma_0^3, \quad (8)$$

$$P^* \equiv \frac{P\sigma_0^3}{U_0}, \quad (9)$$

$$D^* \equiv \frac{D(m/U_0)^{1/2}}{\sigma_0}, \quad (10)$$

and

$$\tau_r^* \equiv \frac{\tau_r(U_0/m)^{1/2}}{\sigma_0}, \quad (11)$$

where  $k_B$  is the Boltzmann constant,  $m$  is the particle mass, and  $U_0$  is the high of the repulsive ramp.

We calculate thermodynamic and dynamic properties using simulations of 160,000 time steps. We analyze the thermodynamic and dynamic behavior for dimensionless temperatures ranging from  $T^*=0.151$  down to  $T^*=0.054$  for  $n=18$  and from  $T^*=0.168$  down to  $T^*=0.048$  for  $n=144$ .

### III. RESULTS

#### A. Density anomaly

We shall first investigate if our system of diatomic molecules exhibits a density maximum, as found for a system of spherical monoatomic particles interacting through the same potential [28]. Figure 2 plots the pressure  $P^*$  against density  $\rho^*$  for fixed values of  $T^*$ . We see that for all the states, there

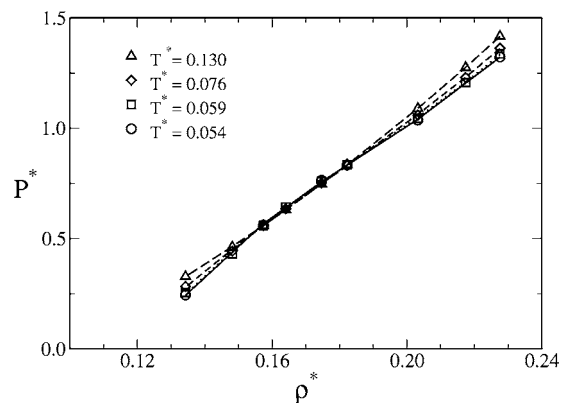


FIG. 2. Dimensionless pressure,  $P^*$ , as a function of dimensionless density,  $\rho^*$ , for four different isotherms in the system with  $n=18$  steps (Fig. 1). Note that the pressure isotherms cross each other (dashed circle), which implies a density anomaly since  $d\rho/dT=0$ .

is no mechanical instability, and the pressure is a monotonically increasing function of density,

$$\left(\frac{\partial P}{\partial \rho}\right)_T > 0, \quad (12)$$

implying that no phase transition is present. The isotherms cross each other, which means that  $(\partial P/\partial T)_\rho=0$ , which implies a density anomaly.

In order to locate the points where  $(\partial P/\partial T)_\rho=0$ , we plot  $P^*$  against  $T^*$  along isochores Figs. 3(a)–3(c), fit the results to a polynomial, and calculate the minima. The line connecting these minima is the temperature of maximum density (TMD) line, which is the boundary of a thermodynamically anomalous region where

$$\left(\frac{\partial P}{\partial T}\right)_\rho < 0, \quad (13)$$

and therefore an anomalous behavior of the density (similar to water)

$$\left(\frac{\partial \rho}{\partial T}\right)_P > 0. \quad (14)$$

Because of the Maxwell relations, Eq. (14) implies anomalous behavior of the entropy,

$$\left(\frac{\partial S}{\partial \rho}\right)_T > 0. \quad (15)$$

We can uncover the effect of increasing  $n$  on generating the thermodynamic and dynamic anomalies, comparing Figs. 3(a) and 3(b). We will see that the number of steps has almost no influence on the shape and location of the TMD, consistent with the fast convergence of pressure to the linear ramp value as  $n \rightarrow \infty$  [28]. Therefore, the curves for the system with  $n=144$  steps are expected to be almost identical to the curves for the linear ramp [26]. The corresponding effect of the dumbbell shape can be estimated by comparing the results of dumbbells with  $n=18$  and  $n=144$  with the systems of 1000 monoatomic particles with  $n=18$  [Fig. 3(c)] and

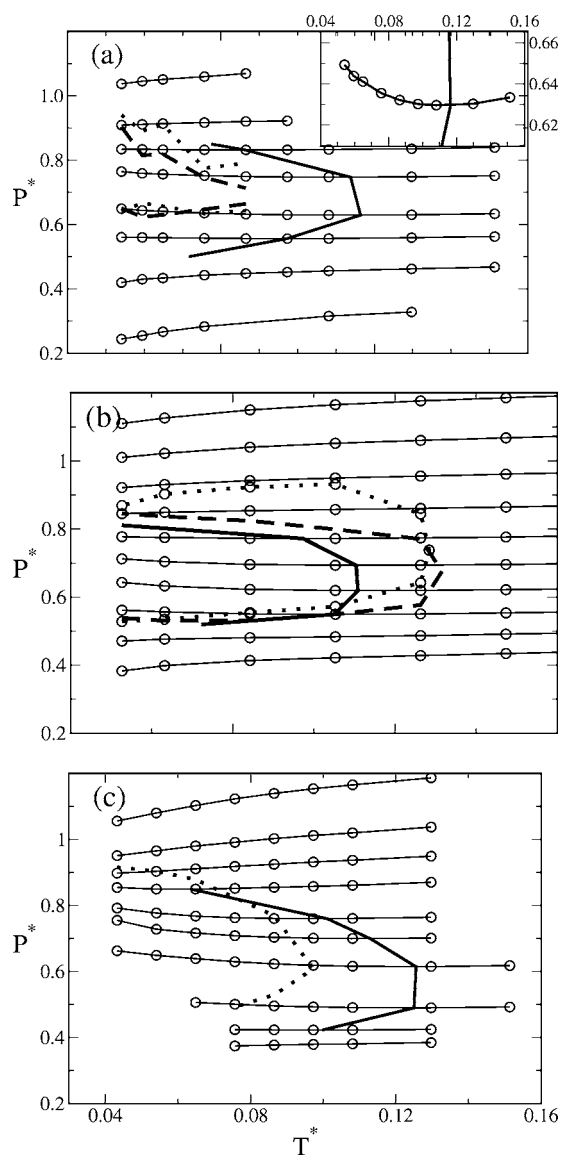


FIG. 3. Dimensionless pressure against dimensionless temperature along isochores. Bold line: TMD line. Dotted line: Boundary of the diffusivity extrema. Dashed line: Boundary of the rotational mobility extrema. (a) Dumbbell molecules interacting via the repulsive discretized ramp  $\rho$  potential with  $n=18$  steps. From top to bottom, densities  $\rho^*=0.203, 0.190, 0.182, 0.175, 0.164, 0.157, 0.148,$  and  $0.134$ . In the inset is shown the density  $\rho^*=0.164$ , in a scale suitable to see the minimum in the pressure. (b) The case of  $n=144$  steps. From top to bottom, densities  $\rho^*=0.208, 0.199, 0.190, 0.182, 0.175, 0.167, 0.161, 0.154, 0.148,$  and  $0.142$ . (c) System of 1000 atoms (without the bonds), with interaction potential with  $n=18$  steps. From top to bottom, densities  $\rho^*=0.406, 0.381, 0.364, 0.349, 0.328, 0.315, 0.296, 0.269, 0.254,$  and  $0.244$ .

$n=144$  [28] interacting with the same potential illustrated in Eq. (3) for the same state points as the dumbbell molecule system. The systems of interacting dumbbells have a slightly smaller region of density (and entropy) anomaly, shifted to higher pressures. In these cases, for densities above 0.182 and below 0.154, no minima in the pressure are found.

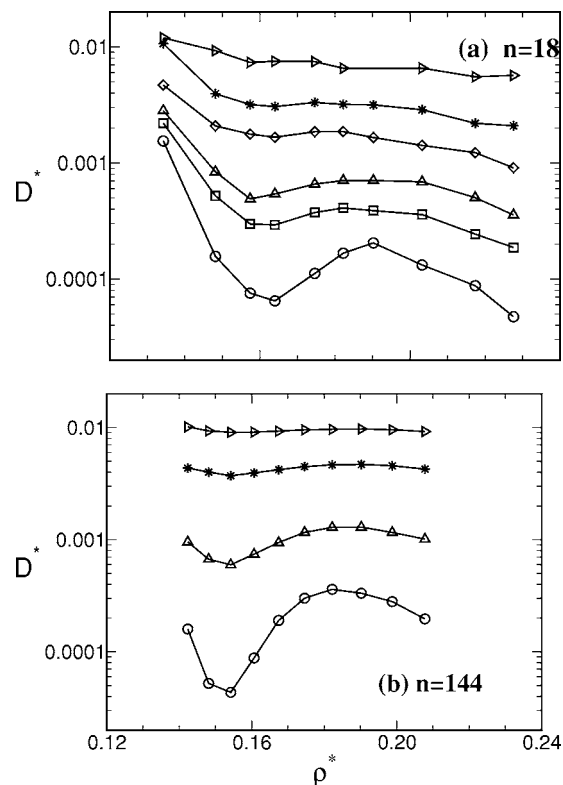


FIG. 4. (a) Diffusion coefficient as a function of density, along six isotherms (from top to bottom  $T^*=0.108, 0.086, 0.075, 0.065, 0.059,$  and  $0.054$ ) for  $n=18$  steps. (b)  $T^*=0.105, 0.084, 0.063,$  and  $0.052$  for  $n=144$  steps.

## B. Dynamics

We now study the mobility associated with the repulsive ramp  $n$ -step potential for  $n=18$  and  $n=144$ . We calculate the translational diffusion coefficient  $D$  using the mean-square displacement averaged over different initial times,

$$\langle \Delta r^2(t) \rangle = \langle [\mathbf{v}(t_0 + t) - \mathbf{r}(t_0)]^2 \rangle, \quad (16)$$

where  $\mathbf{v}$  is the center of mass of the dumbbell. Then  $D$  is obtained from the relation

$$D = \lim_{t \rightarrow \infty} \langle \Delta r^2(t) \rangle / 6t. \quad (17)$$

Figure 4 shows the behavior of the dimensionless translational diffusion coefficient,  $D^*$ , as a function of the dimensionless density,  $\rho^*$ , for the dumbbell potential. At low temperatures, the behavior is similar to the behavior found for SPC/E supercooled water [11].  $D$  increases as  $\rho$  decreases, reaches a maximum at  $\rho_{D \max}$  (and  $P_{D \max}$ ), and decreases until it reaches a minimum at  $\rho_{D \min}$  (and  $P_{D \min}$ ). Above  $T^*=0.086$ , however, the anomalous behavior disappears.

The region in the  $P$ - $T$  plane where there is an anomalous behavior in the diffusion is bounded by  $[T_{D \min}(\rho), P_{D \min}(\rho)]$  and  $[T_{D \max}(\rho), P_{D \max}(\rho)]$ . The location of this region for the studied systems is shown by the dotted lines in Figs. 3(a)–3(c). The effect of the dumbbell shape observed by comparing Figs. 3(a) and 3(c), or Fig. 3(b) and Ref. [28], is rather small and affects only the overall shape of the curve,

slightly shrinking the region and shifting toward higher values of  $P$  and lower values of  $T$ . The effect of  $n$ , obtained by comparing Figs. 3(a) and 3(b) or Fig. 3(c) and Ref. [28], however, is very strong. Whereas in the systems where the potential was discretized in 144 steps (Fig. 3(b) and Ref. [28]) the diffusion anomaly line lies outside the TMD line (exactly as in SPC/E water [38]), for the systems with  $n=18$  [Figs. 3(a) and 3(c)], the diffusion anomaly region shrinks strongly, in such a way that it migrates to a region inside the TMD line, in contrast to the behavior of SPC/E water. These results are consistent with the slow convergence of the dynamic properties of the discretized ramp potential, as  $n \rightarrow \infty$ . Nevertheless, the results for  $n=144$  are expected to be very similar to the results for a linear ramp.

The use of dumbbell molecules, unlike spherically symmetric models, allows us to calculate the rotational degrees of freedom and to estimate the role of anisotropy. The rotational diffusion is analyzed by calculating the orientational autocorrelation function of the vector  $\mathbf{e}(t)$  defining the orientation of the dumbbell molecule,

$$C_{\mathbf{e}}(t) \equiv \langle \mathbf{e}(t) \cdot \mathbf{e}(0) \rangle. \quad (18)$$

The orientational autocorrelation function depends on the density and temperature, and for short times we can fit  $C_{\mathbf{e}}(t)$  with an exponential function [42]:

$$C_{\mathbf{e}}(t) \propto \exp(-t/\tau_r). \quad (19)$$

The orientational correlation times,  $\tau_r$ , obtained from Eq. (19) depends on density in a roughly complementary way as the translational diffusion coefficient  $D$ . This behavior is shown in Figs. 5(a) (for the  $n=18$  system) and 5(b) (for the  $n=144$  system).

As  $\rho$  decreases,  $\tau_r$  decreases, reaches a minimum, then increases, reaching a maximum. A similar behavior was also observed for SPC/E water simulations [30–32]. The density region where the rotational diffusion is anomalous roughly coincides with the region of translational diffusion anomalies, as seen in Figs. 3(a) and 3(b) (dashed lines). Here again, the anomaly region depends strongly on  $n$ .

The translational and rotational diffusion for systems for the  $n$ -step repulsive ramp seem to behave in a complementary way, but in fact the product  $\tau_r D$ , as shown in Fig. 6(a), is not density or temperature independent as in SPC/E water [30–32]. Indeed,  $\tau_r D$  increases with increasing temperature [Fig. 6(b)], in sharp contrast with most liquids. Inside the thermodynamically anomalous region, the product  $\tau_r D$  is also not a constant, and a careful examination of the very low-temperature behavior [Fig. 6(b)] shows that the product increases upon cooling below  $T^*=0.048$ , in a way similar to many other systems close to the glass transition temperature [37]. For our systems, we estimate the mode coupling temperature (MCT) to be  $T_{\text{MCT}}^*=0.044 \pm 0.001$  and using the Vogel-Fulcher ansatz  $D \propto \exp[A/(T-T_0)]$ , we estimate  $T_0^*=0.038 \pm 0.001$ . The glass transition temperature is between these two values.

The explanation for the anomalous behavior of the product  $\tau_r D$  is that the rotation of the dumbbell in the vicinity of other dumbbells may have a different activation energy than translation. This is quite plausible from

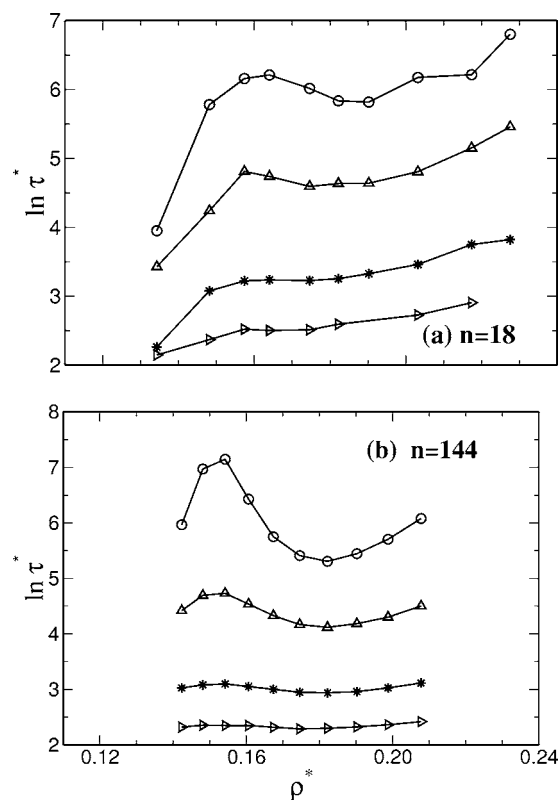


FIG. 5. (a) Orientational time as a function of density for four isotherms (from bottom to top  $T^*=0.108, 0.086, 0.065$ , and  $0.054$ ) for  $n=18$  steps (b)  $T^*=0.105, 0.084, 0.063$ , and  $0.052$  for  $n=144$  steps.

simple geometrical considerations. In order to rotate, the dumbbell must overcome a larger potential barrier than to translate. Then,  $\ln \tau_r D = (A_r - A_t)/kT$ , where both  $A_r$  and  $A_t$  should be functions of density. Indeed the Arrhenius plot of  $\tau_r D$  at high and moderate temperatures gives perfect straight lines with weak dependence on density [Fig. 6(b)]. Figure 7 shows that  $A_r - A_t$ , which quantifies how strongly the product  $\tau_r D$  deviates from a constant, reaches its maximum close to the density corresponding to the closed-packed arrangements of the rumps, below which the dumbbells may translate without overcoming any potential barrier. This density may be estimated for an arrangement of dumbbells consisting of triangular lattices of vertically placed dumbbells  $\rho = 1/(\sigma_1^3/\sqrt{2} + \sigma_1^2\sigma_0\sqrt{3}/2) = 0.153\sigma_0^{-3}$ , where  $\sigma_0$  is the hard core and  $\sigma_1$  is considered a soft core diameter. The linearity of the Arrhenius plot breaks down close to the glass transition, where  $\tau_r D$  starts to increase upon cooling as in other liquids in which this behavior is usually associated with the breakdown of the Einstein-Stokes caused by the growth of dynamic heterogeneities near the glass transition [35,37,44].

#### IV. CONCLUSIONS

We have simulated a set of dumbbell molecules interacting through a purely repulsive ramplike potential, discretized in  $n$  steps. We compare the cases of  $n=18$  and  $n=144$ , where the  $n=144$  case has behavior very similar to that of the linear

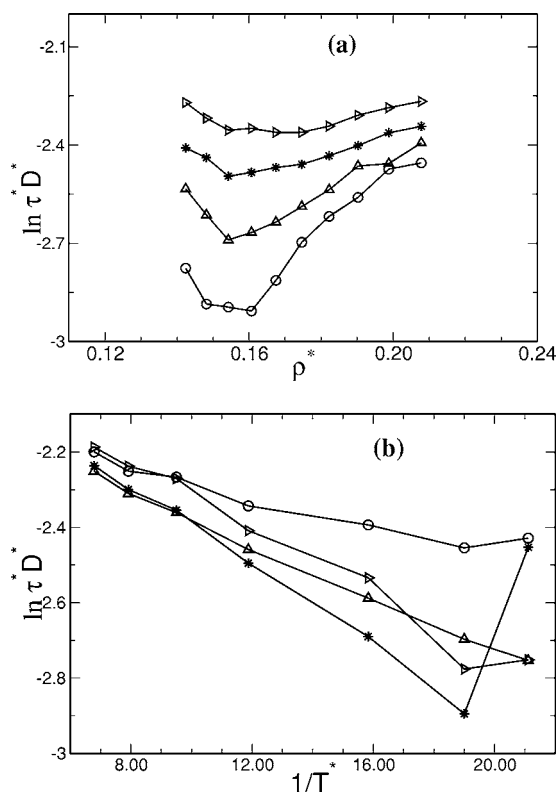


FIG. 6. (a) Product  $\tau_r D^*$  as a function of density for four isotherms (from top to bottom  $T^* = 0.105, 0.084, 0.063,$  and  $0.052$ ) for  $n=144$  steps (b) Product  $\tau_r D^*$  as a function of the inverse of temperature along isochores for  $n=144$  steps (circles:  $\rho=0.208$ , up triangles:  $\rho=0.175$ , stars:  $\rho=0.154$ , right triangles:  $\rho=0.142$ ).

ramp. We studied the density anomaly and anomalies in both the translational and rotational mobilities. We found that in both cases the density behaves anomalously in a certain range of pressures and temperatures. Comparison with simulations of monoatomic particles interacting with the same potential [28] shows that the thermodynamic anomalies are not very sensitive to the number of steps used in the potential, and only weakly affected by the dumbbell shape. Thus, the existence of a fixed link between pairs of atoms and the resulting anisotropy has only a small effect on the thermodynamic properties.

The dynamic anomalies, however, are more sensitive, both to  $n$  and to the introduction of the dumbbell shape. The translational diffusion coefficient at constant temperature has a maximum and a minimum as a function of  $\rho$ , but the locus of anomalous behavior depends both on the particles' shape (monoatomic or dumbbell) as well as on the number of steps (a potential with 144 steps has a different range than a potential with 18 steps). The dumbbell shape causes the dynamically anomalous region to shrink. The decrease of  $n$  shrinks and shifts the dynamically anomalous region to lower temperatures.

The discretization (number of steps,  $n$ ) has, therefore, a much stronger effect on the dynamic anomalies than on the thermodynamic anomalies in such a way that the locus of the anomalies can change dramatically. This can be understood

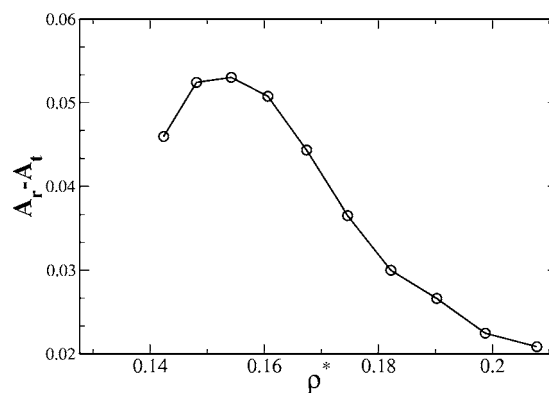


FIG. 7. Difference between the rotational and translational activation energies,  $A_r$  and  $A_t$ , calculated as a function of density from the product  $\tau_r D$ .

as follows: The thermodynamic properties sampled in a DMD simulation for a potential discretized in  $n$  steps converge to the continuous values as  $1/n^2$  [28]. On the other hand, the dynamics depend on the size of the jump, which scales as  $1/n$ , which explains the stronger effect on the dynamics. Due to the ability of the model to shift the anomalous region, it could potentially describe and unite a spectrum of network-forming fluids depending on the “ruggedness” of the pairwise potential.

The region of dynamic anomalies lies approximately inside the region of thermodynamic anomalies for the  $n=18$  potential and outside for the  $n=144$  potential. We expect that systems with molecules interacting with a smooth linear ramp potential would display a behavior similar to this last one. Despite the fact that this last hierarchy of anomalous regions is similar to that found in simulations of water, some important differences should be pointed out. For dumbbell molecules, the product of the translational diffusion constant  $D$  and the orientational correlation time  $\tau_r$  is not a constant, even at high temperatures, indicating that translation and rotation of dumbbells may have different activation energies. This is not the case in water in which the molecules are confined in symmetrical tetrahedral shells, so the translation and rotation are associated with switching the partners via bifurcation of the hydrogen bonds [30]. It would be interesting to compare the behavior of the  $\tau_r D$  in the dumbbell model and other dimeric liquids, such as hydrogen peroxide. At low temperatures, the dumbbell model displays a sharp increase of  $\tau_r D$ , resembling the behavior found for liquids close to  $T_g$  [37]. This behavior must be investigated by analyzing the “fastest” rotational and translational clusters [43–45].

#### ACKNOWLEDGMENTS

We thank P. Kumar for helpful insights and comments on the manuscript, and the Brazilian science agencies CNPq, FINEP, and Fapergs, and by the NSF Chemistry Program for financial support. One of the author (S.V.B.) thanks the office of Academic affairs of the Yeshiva University for financial support.

- [1] For a recent review, see P. Debenedetti, *J. Phys.: Condens. Matter* **15**, R1669 (2003); S. V. Buldyrev, G. Franzese, N. Giovambattista, G. Malescio, M. R. Sadr-Lahijany, A. Scala, A. Skibinsky, and H. E. Stanley, *Physica A* **304**, 23–42 (2002).
- [2] E. A. Jagla, *Phys. Rev. E* **58**, 1478 (1998); *J. Chem. Phys.* **110**, 451 (1999); **111**, 8980 (1999); *Phys. Rev. E* **63**, 061501 (2001); **63**, 061509 (2001).
- [3] M. R. Sadr-Lahijany, A. Scala, S. V. Buldyrev, and H. E. Stanley, *Phys. Rev. Lett.* **81**, 4895 (1998); M. R. Sadr-Lahijany, A. Scala, S. V. Buldyrev, and H. E. Stanley, *Phys. Rev. E* **60**, 6714 (1998).
- [4] A. Scala, M. R. Sadr-Lahijany, N. Giovambattista, S. V. Buldyrev, and H. E. Stanley, *J. Stat. Phys.* **100**, 97 (2000); A. Scala, M. R. Sadr-Lahijany, N. Giovambattista, S. V. Buldyrev, and H. E. Stanley, *Phys. Rev. E* **63**, 041202 (2001).
- [5] G. Franzese, G. Malescio, A. Skibinsky, S. V. Buldyrev, and H. E. Stanley, *Nature (London)* **409**, 692 (2001).
- [6] S. V. Buldyrev, G. Franzese, N. Giovambattista, G. Malescio, M. R. Sadr-Lahijany, A. Scala, A. Skibinsky, and H. E. Stanley, *Physica A* **304**, 23 (2002).
- [7] G. Franzese, G. Malescio, A. Skibinsky, S. V. Buldyrev, and H. E. Stanley, *Phys. Rev. E* **66**, 051206 (2002); A. Skibinsky, S. V. Buldyrev, G. Franzese, G. Malescio, and H. E. Stanley, *ibid.* **69**, 061206 (2004).
- [8] N. B. Wilding and J. E. Magee, *Phys. Rev. E* **66**, 031509 (2002).
- [9] P. J. Camp, *Phys. Rev. E* **71**, 031507 (2005).
- [10] *Water: A Comprehensive Treatise*, edited by F. Franks, (Plenum, N.Y., 1972), Vols. 1–7; *Water Science Reviews* (Cambridge University Press, Cambridge, UK, 1985), Vols. 1–4.
- [11] P. A. Netz, F. W. Starr, H. E. Stanley, and M. C. Barbosa, *J. Chem. Phys.* **115**, 344 (2001).
- [12] M. G. Campos and J. R. Grigera, *Mol. Simul.* **30**, 537 (2004).
- [13] P. H. Poole, F. Sciortino, U. Essmann, and H. E. Stanley, *Nature (London)* **360**, 324 (1992); *Phys. Rev. E* **48**, 3799 (1993); F. Sciortino, P. H. Poole, U. Essmann, and H. E. Stanley, *ibid.* **55**, 727 (1997); S. Harrington, R. Zhang, P. H. Poole, F. Sciortino, and H. E. Stanley, *Phys. Rev. Lett.* **78**, 2409 (1997). For a review, see O. Mishima and H. E. Stanley, *Nature (London)* **396**, 329 (1998).
- [14] P. C. Hemmer and G. Stell, *Phys. Rev. Lett.* **24**, 1284 (1970); G. Stell and P. C. Hemmer, *J. Chem. Phys.* **56**, 4274 (1972); J. M. Kincaid, G. Stell, and C. K. Hall, *ibid.* **65**, 2161 (1976); J. M. Kincaid, G. Stell, and E. Goldmark, *ibid.* **65**, 2172 (1976); C. K. Hall and G. Stell, *Phys. Rev. A* **7**, 1679 (1973).
- [15] H. Takahashi, E. H. Lieb, and D. C. Mattis, *Mathematical Physics in One Dimension* (Academic, New York, 1966).
- [16] P. G. Debenedetti, V. S. Raghavan, and S. S. Borick, *J. Phys. Chem.* **95**, 4540 (1991).
- [17] F. H. Stillinger and D. K. Stillinger, *Physica A* **244**, 358 (1997).
- [18] S. V. Buldyrev, G. Franzese, N. Giovambattista, G. Malescio, M. R. Sadr-Lahijany, A. Scala, A. Skibinsky, and H. E. Stanley, in *New Kinds of Phase Transitions: Transformations in Disordered Substances*, NATO Advanced Research Workshop, Volga River, edited by V. Brazhkin, S. V. Buldyrev, V. N. Ryzhov, and H. E. Stanley (Kluwer, Dordrecht, 2002), p. 97.
- [19] S. V. Buldyrev and H. E. Stanley, *Physica A* **330**, 124 (2003).
- [20] A. Skibinsky, S. V. Buldyrev, G. Franzese, G. Malescio, and H. E. Stanley, *Phys. Rev. E* **69**, 061206 (2004).
- [21] C. H. Cho, S. Singh, and G. W. Robinson, *Phys. Rev. Lett.* **76**, 1651 (1996).
- [22] C. H. Cho, S. Singh, and G. W. Robinson, *Faraday Discuss.* **103**, 19 (1996).
- [23] V. B. Henriques and M. C. Barbosa, *Phys. Rev. E* **71**, 031504 (2005); V. B. Henriques, N. Guisoni, M. A. Barbosa, M. Thielo, and M. C. Barbosa, *Mol. Phys.* **103**, 3001 (2005).
- [24] A. B. de Oliveira, P. A. Netz, T. Colla, and M. C. Barbosa, *J. Chem. Phys.* **124**, 84505 (2006); A. B. de Oliveira and M. C. Barbosa, *J. Phys.: Condens. Matter* **17**, 399 (2005); A. L. Baladares and M. C. Barbosa *ibid.* **16**, 8811 (2004).
- [25] G. Malescio, G. Franzese, A. Skibinsky, S. V. Buldyrev, and H. E. Stanley, *Phys. Rev. E* **71**, 061504 (2005).
- [26] H. M. Gibson and N. B. Wilding, cond-mat/0601474.
- [27] F. J. Rogers and D. A. Young, *Phys. Rev. A* **30**, 999 (1984).
- [28] P. Kumar, S. V. Buldyrev, F. Sciortino, E. Zaccarelli, and H. E. Stanley, *Phys. Rev. E* **72**, 021501 (2005).
- [29] L. Xu, P. Kumar, S. V. Buldyrev, S.-H. Chen, P. H. Poole, F. Sciortino, and H. E. Stanley, *Proc. Natl. Acad. Sci. U.S.A.* **102**, 16558 (2005).
- [30] P. A. Netz, F. W. Starr, M. C. Barbosa, and H. E. Stanley, *Physica A* **314**, 470 (2002).
- [31] H. E. Stanley, M. C. Barbosa, S. Mossa, P. A. Netz, F. Sciortino, F. W. Starr, and M. Yamada, *Physica A* **315**, 281 (2002).
- [32] P. A. Netz, F. W. Starr, M. C. Barbosa and H. E. Stanley, *J. Mol. Liq.* **101**, 159 (2002).
- [33] H. J. C. Berendsen, J. R. Grigera, and T. P. Shaatsma, *J. Phys. Chem.* **91**, 10269 (1987).
- [34] F. Ould-Kaddour and D. Levesque, *Phys. Rev. E* **63**, 011205 (2000).
- [35] K. L. Ngai, *J. Phys. Chem. B* **103**, 10684 (1999).
- [36] F. Fujara, H. Geil, H. Sillescu, and G. Fleischer, *Z. Phys. B: Condens. Matter* **88**, 195 (1992).
- [37] M. T. Cicerone, F. R. Blackburn, and M. D. Ediger, *J. Chem. Phys.* **102**, 471 (1995); M. T. Cicerone and M. D. Ediger, *ibid.* **104**, 7210 (1996).
- [38] J. R. Errington and P. G. Debenedetti, *Nature* **409**, 318 (2001).
- [39] Z. Yan, S. V. Buldyrev, N. Giovambattista, and H. E. Stanley, *Phys. Rev. Lett.* **95**, 130604 (2005).
- [40] Z. Yan, S. V. Buldyrev, N. Giovambattista, P. G. Debenedetti, and H. E. Stanley (unpublished).
- [41] D. C. Rapaport, *The Art of Molecular Dynamics Simulation* (Cambridge University Press, Cambridge, U.K., 1995).
- [42] The number of points included in the fit depends on temperature: We took as cutoff for the exponential region the largest time before the autocorrelation function become smaller than its fluctuations.
- [43] J. Kim and T. Keyes, *J. Chem. Phys.* **121**, 4237 (2004).
- [44] M. G. Mazza, N. Giovambattista, F. W. Starr, and H. E. Stanley, *Phys. Rev. Lett.* **96**, 057803 (2006).
- [45] Y.-J. Jung, J. P. Garrahan, and D. Chandler, *Phys. Rev. E* **69**, 061205 (2004).